

Nanosatellites Technology Demonstration

Ángel Martínez (1), Ignacio Arruego (2), Maria Teresa Álvarez (3), Jesús Barbero (4), Héctor Guerrero (5), David Levy (6), Ana Gras (7)

Instituto Nacional de Técnica Aeroespacial “Esteban Terradas” (INTA)
Carretera Torrejón-Ajalvir Km.4, P.O. 28850, Torrejón de Ardoz,
Madrid, Spain

(1) División de Ciencias del Espacio, +34 915 201 655, martinezja@inta.es

(2) División de Ciencias del Espacio, +34 915 201 655, arruegori@inta.es

(3) División de Ciencias del Espacio, +34 915 201 740, alvarezat@inta.es

(4) División de Ciencias del Espacio, +34 915 201 740, barberosj@inta.es

(5) División de Ciencias del Espacio, +34 915 202 152, guerreroph@inta.es

(6) División de Ciencias del Espacio, +34 915 201 847, levycd@inta.es

(7) Departamento de Ensayos Electrónicos; SPASOLAB (SPAcE SOLar testing LABoratory), +34 915 201 355, grassa@inta.es

Abstract. Nowadays, it is widely used the term Nanosatellite when we refer to those satellites whose mass are less than about 10 kg. But it is not only a question of size and power consumption when we talk about this new kind of satellites; it is also a new spacecraft design philosophy. In this paper, we present a small LEO (Low Earth Orbit) satellite, named ‘NANOSAT’, designed and developed by the Spanish Space Agency INTA (Instituto Nacional de Técnica Aeroespacial), currently in the manufacturing and testing phase. We will show here the general design philosophy, which has conducted the project to this stage, giving a description of each subsystem inside the satellite as well as the interfaces between them.

Introduction

Small satellites have literally been around since the dawn of the Space Age. Small, cheap satellites used to be an exclusive domain of scientific and amateur groups. But now, major advances in microelectronics, especially microprocessors have made of small satellites a viable alternative. They provide cost-effective solutions to traditional problems at a time when space budgets are decreasing.

We present here ‘NANOSAT’, a small LEO (Low Earth Orbit) satellite designed and developed by the Spanish Space Agency INTA (Instituto Nacional de Técnica Aeroespacial), currently in the manufacturing and testing phase. The planned satellite will have a near polar orbit in order to survey the entire surface of the Earth and communicate different earth stations placed all around our planet.

The satellite main objective is to prove the feasibility of micro and nanotechnologies implemented in the solar and magnetic sensors in the space environment. The satellite also intends to allow digital transmission of data between remote scientific stations all around the Earth and a Central Station using store-and-forward communication techniques. The communication subsystem tries to follow the ‘software radio’ point of view. It uses a CPM modulation of the GMSK type together with efficient

carrier and bit synchronization techniques in the receiver.

Low cost implementation has been a constraint and consequently we have avoided the use of radiation resistant integrated circuits for all but the critical functions of the satellite. Screened commercial and military standards have been considered in combination with some additional shielding. Some of the integrated circuits (ICs) like the DSP (Digital Signal Processor) have been ground radiation tested in order to evaluate the error rate under harsh space conditions.

NANOSAT Architecture

We can see in figure 1 a general block diagram for our nanosatellite.

It includes the most important subsystems inside the satellite, which are:

1. Power Unit: the power distribution unit (PDU) includes the solar panels, built with GaAs solar cells, the batteries and the necessary electronic to generate and distribute the power supply. This unit generates the necessary voltage with some DC/DC converters based on a main bus of at least 18 V, which supplies to each subsystem through a star shaped configuration. We use twisted pair wires with ground.

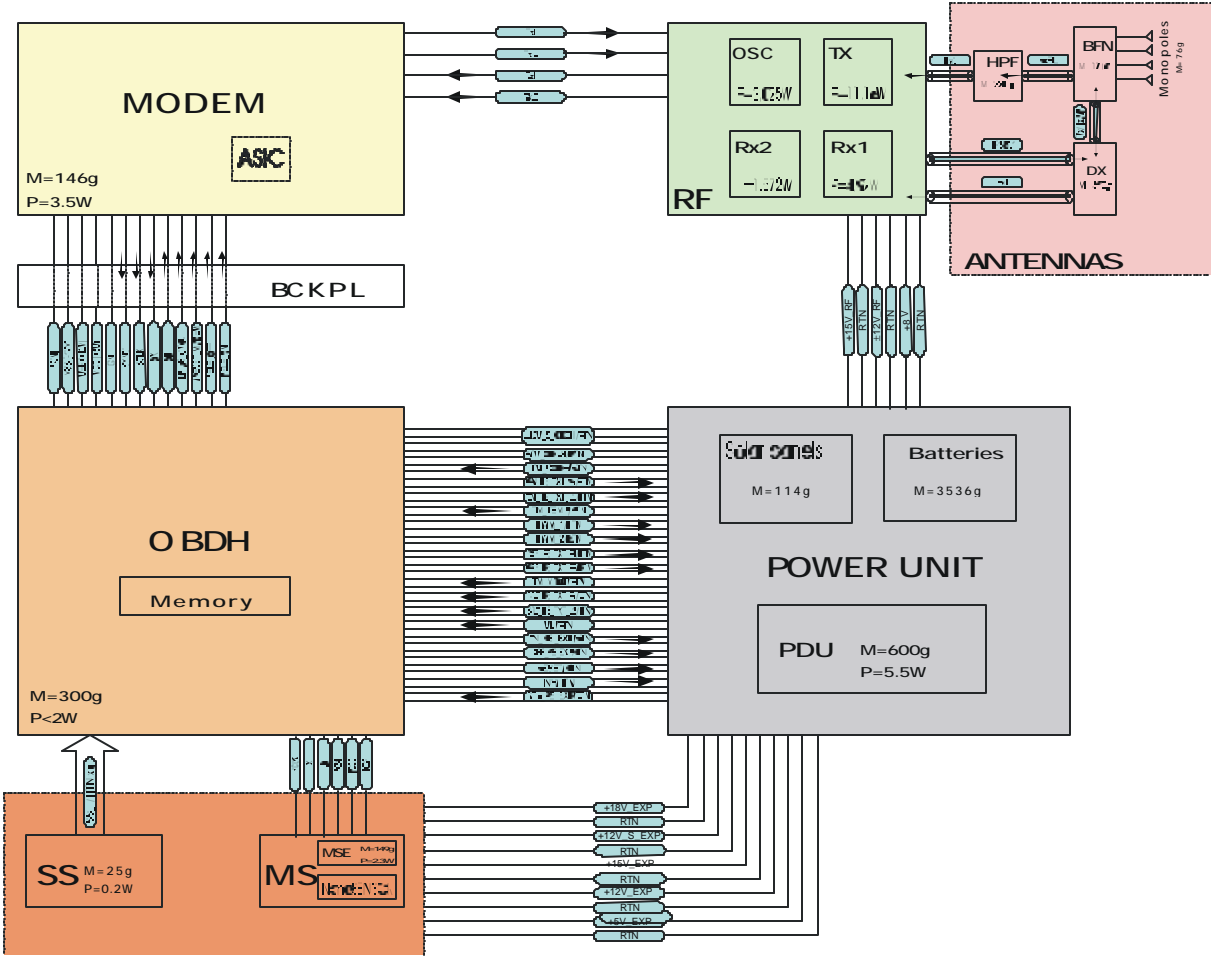


Figure 1. NANO-SAT architecture

Three different power groups can be distinguished as a function of the target subsystem:

- RF subsystem and antennas.
- OBDH.
- Experiments (solar and magnetic sensors).

There is also a control interface with the OBDH to carry out telemetry functions of the batteries and solar panels status, as well as to switch on and off some of the subsystems, thus optimizing power consumption.

2. OBDH: it is the central processing unit of the satellite. It stores and processes the data sent and received from the communication subsystems (through a serial interface physically implemented with a backplane) as well as the data incoming from the experiments (interface with the solar and magnetic sensors interface) and the Power Distribution Unit. It also implements the communication protocol, ephemerides control, etc.

3. Modem: the digital modem in NANO-SAT is based on a GMSK modulation, and transmits the incoming data from the OBDH to the earth stations. It implements digital channel coding techniques to improve the bit error rate. All the synchronization functions have also been digitally implemented. It is power supplied through a backplane shared with the OBDH. The modem main functions have been implemented on a DSP (Digital Signal Processor). There is also a redundant ASIC in case there is a problem with the DSP.

4. RF and antennas subsystem: it modulates and demodulates the in-quadrature components of the baseband signal. It includes an intermediate frequency stage at 70 MHz, as well as the necessary clock oscillators to up-convert and down-convert the signal to its final frequency (from baseband to 387.1 MHz for the up-conversion and from 400 to 70 MHz for the down-conversion). The High Power Amplifier (HPA) output is introduced to the Beam Forming Network (BFN), which feeds 4 monopoles to

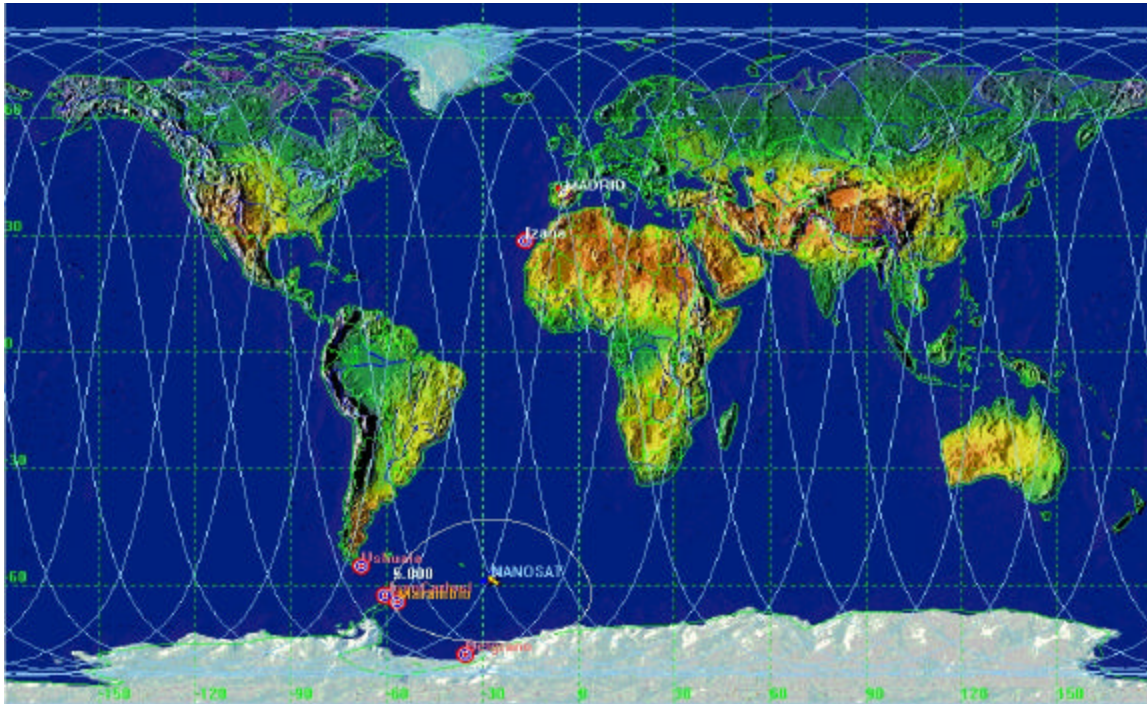


Figure 2. Earth Stations and NANOSAT tracking. 5 degrees elevation contour shown

generate a circular polarization. It also includes four printed circuit boards (PCB): one for the oscillators, another for the transmission chain and two more for the reception components. A diplexer allows to share the antenna between the two paths.

5. Experiments: this block includes a two axis magnetic sensor and six solar sensors placed on some of the satellite faces. The magnetic sensor communicates with the OBDH through a serial port, whereas the solar sensors use analog interfaces with the OBDH, which will need analog-to-digital converters to process the received data.

Mission Analysis

NANOSAT is a satellite intended to achieve three objectives. The first one is to develop a space platform to allow the experimentation in the space environment of some new micro and nanotechnologies.

In this sense, there are two different experiments within the present mission to be taken aboard NANOSAT: the nano-solar-sensor and the nano-magnetic-sensor. For the future, this is the basis to be able to develop low-cost nano-satellites ad hoc for any kind of in-orbit testing of new micro and nano devices.

The second objective has to do with the application, and it is to allow store-and-forward communications, including a mailing service, between remote scientific stations and a Central Station placed in Madrid. INTA has scientific equipment for atmospheric studies in the Antarctica (Ushuaia, Marambio, Belgrano, Juan Carlos I) and in the Canary Islands (Izaña). NANOSAT will belong to an owner system that communicates remote stations between them and with the Central Station in order to allow data transmission during long winter periods when there is nobody there.

Finally, NANOSAT will allow in-orbit qualification of some commercial and military components being used in this design.

Due to the fact that most of the earth stations are placed in high latitudes, the satellite orbit must be quasi-polar. In fact, its inclination is almost 98 degrees, with a sun-synchronous orbit at 645-km. Therefore, the satellite completes a revolution in about 97 minutes. The low earth orbit reduces the necessary transmitted power to allow communications, which is an improvement from the link-budget point of view. Moreover, a sun-synchronous orbit with eclipse is desirable in order to facilitate thermal control with no active elements. Taking everything into account, the selected orbit is the best fitted to our mission.

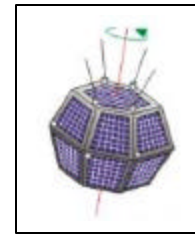
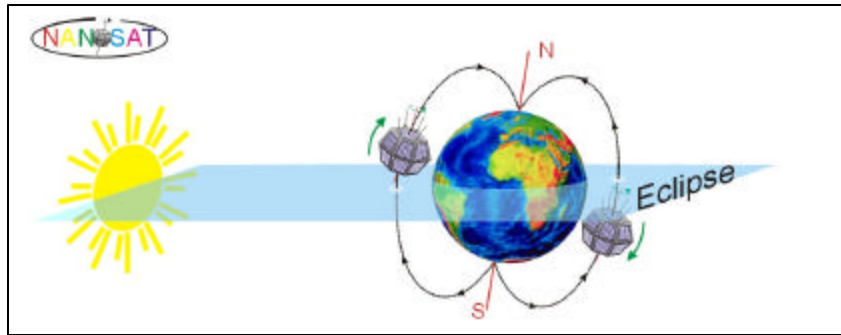


Figure 3. NANOSAT orbit and spin orientation

According to NANOSAT philosophy, all the non-essential elements have been suppressed. Both an active attitude control and pointing system have been avoided by using omni-directional antennas and having no elements (sensors) that could need some kind of pointing or positioning. The satellite will spin around its main inertial-momentum axis and will be passively orientated according to the Earth spinning axis. Therefore, thermal control is carried out with thermal conducts instead of active elements.

The solar cells will be attached to the satellite structure, thus avoiding the need for solar panels and the necessary deployment system.

Finally, NANOSAT structure will be composed of two hemispheres that can be separated in order to increase internal access. Each part has one hexagonal and six trapezoidal shaped sides, being the junction of the hemispheres in the equatorial plane of the satellite. This shape approximates, with planar sides easily manufactured, an sphere, which is the shape that maximizes the relationship between surface and volume, reduces the atmospheric friction that still exists at that height and it is the one that best distributes mechanical stresses.

On Board Data Handling

The On Board Data Handling Subsystem (OBDH) is based on the main central processing unit of NANOSAT, and it has to control all the tasks inside the satellite.

The OBDH is electrically connected to each of the other satellite subsystems, as shown in figure 4:

- Communication subsystem.
- Experiments.
- Power supply subsystem.
- Electrical Ground Support Equipment (EGSE).

Communications are based on store-and-forward techniques. Therefore, the OBDH includes the necessary memory to store the information received from the different earth stations. Moreover, the OBDH integrates and supports several scientific experiments shown below.

In this way, the OBDH is the heart of the satellite, controlling scientific data, housekeeping and information about the different subsystems. It must

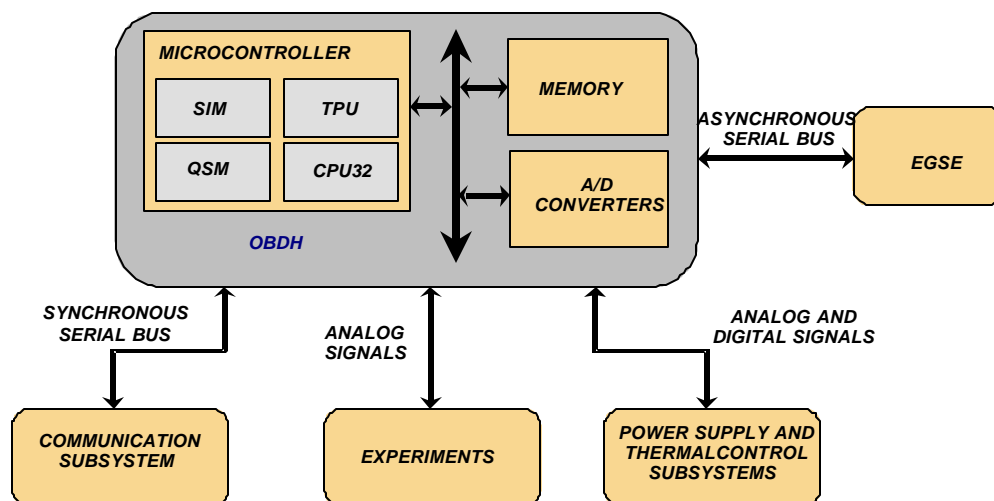


Figure 4. Centralized architecture of the satellite subsystems

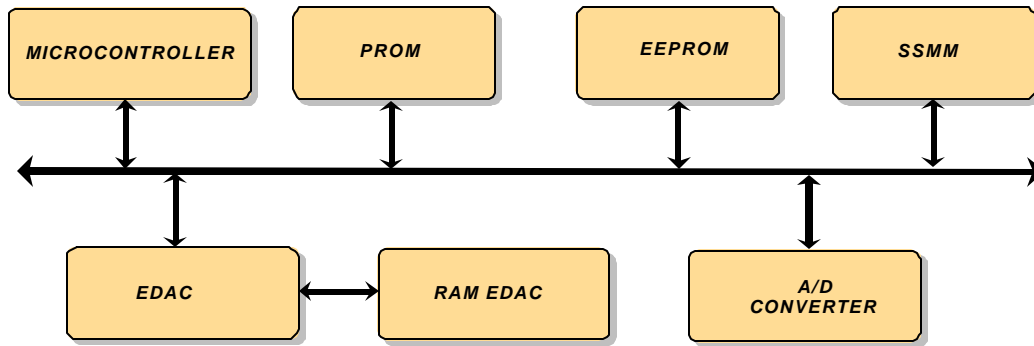


Figure 5. OBDH block diagram

process the incoming data from the experiments, as well as control the power supply unit and store the data received from the earth stations once the communication link has been established. But the OBDH must also carry out those tasks connected with its own operation, such as memory management.

OBDH architecture

Mass, size and power consumption constraints must be fulfilled. As a result, integrated circuits based on CMOS technology have been used. We have chosen the MC68332 micro controller, from Motorola, connected to high storage capacity memories. We can see in figure 5 the OBDH block diagram.

The PROM and EPROM memories have the program code and the operating system. The RAM memory is used to store data of any type, or to execute the program code loaded from the PROM or the EPROM. The storage capacity of the memory area is shown in figure 6.

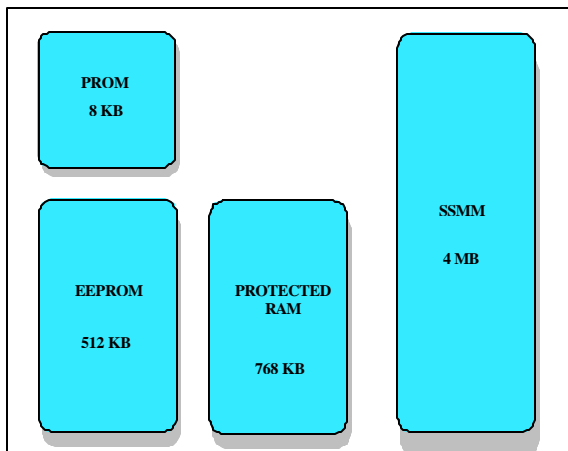


Figure 6. Memory area

Once the satellite has been separated from the launcher, the OBDH is power supplied and the boot loader inside the PROM is executed. When the micro controller is running and the peripherals have been initialized, the program code stored in the EEPROM is copied to the protected RAM for a faster execution.

The EEPROM memories placed on the OBDH allow the system to reload software sent from the Central Earth Station if we want to add new features to our system.

The RAM memory has two difference areas. The SSMM (System Storage Mass Memory) stores the data received from the experiments and the earth stations, as well as housekeeping data. The second area is protected with a modified Hamming code, and stores useful data for the computer or the satellite operation. This memory area is protected with EDAC (Error Detection and Correction) devices, which generate extra bits to be stored together with the data in this memory. These extra bits allow the OBDH to detect and correct a limited number of errors when we read the stored data.

The OBDH has two serial communication ports integrated into the MC68332 microprocessor. The synchronous one is full duplex, and connects the OBDH to the communication subsystem using the Motorola QSPI™ protocol. On the other hand, we can use an asynchronous serial port if we want to configure the transmission data rate and message format.

The A/D converter receive the signal which comes from the solar sensors and sends it in a digital format to the OBDH to be processed.

All the electronic components within the OBDH subsystem must be military qualified. However, some critical components for the system are hardened against space radiation.

NANOSAT Communication Subsystem

Communication systems based on LEO satellites have become more attractive since few years ago. Scientific and military developments, but also commercial applications in the field of personal and mobile communications based on such systems are now a reality. Lower cost on the launching than the

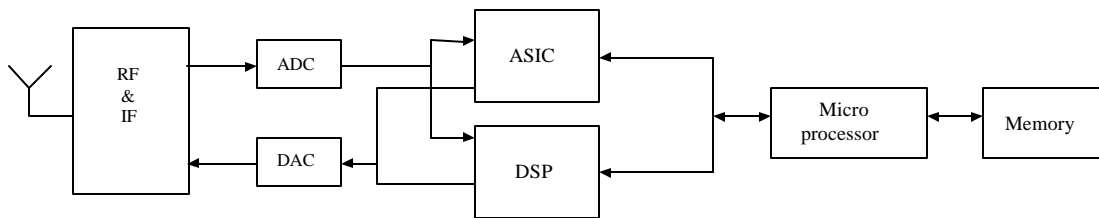


Figure 7. Communication system block diagram

traditional big GEO satellites has a great impact on the overall satellite cost, especially for the very small ones, such as NANOSAT.

A Continuous Phase Modulation of the GMSK type has been used. This modulation is robust to the non-linearity of the power amplifiers and is also bandwidth efficient. The GMSK modulator has been implemented via software on a DSP with look-up tables, whereas we used a linear demodulator based on the linear approximation of CPM modulations¹. Error control is achieved with convolutional encoding, using a soft-decoding scheme based on the Viterbi algorithm.

Digital signal processing techniques have been used for both the onboard modem and the data collection station modems. As a general strategy we use the 'software radio' point of view trying to reduce the analog components and making a digital implementation based on commercial available DSP.

The DSP implements the physical layer, whereas the microprocessor inside the OBDH carries out the higher level protocols of the communication system. Both devices are connected through the DSP and the microprocessor serial ports. The main functions (filtering, bit and carrier synchronization, channel coding/decoding of the modulator/demodulator) are carried out digitally with optimized software algorithms for real-time implementation.

Communication Channel

As we will see, we use a carrier frequency of 400 MHz for the earth stations-satellite link (upward link) and another one of 387 MHz for the downward link (satellite-earth stations). The channel is strongly influenced by a Doppler effect that varies from -10 kHz to $+10$ kHz at those frequencies. This Doppler also changes with time at a maximum rate of ± 120 Hz/s.

In addition, the channel shows an attenuation which changes with satellite-earth station relative position, and this attenuation can change in about 15 dB. We

also have to take into account the typical fading present in satellite communications.

Taking into account the time-varying nature of the channel, we decided to implement training strategies accordingly to modem parameters. Tuning the bit rate, for example, is particularly effective in order to increase the throughput in the time interval that the channel introduces lower attenuation and Doppler.

Architecture Overview

Figure 7 shows the general architecture of communication subsystem. There is an RF and IF block which includes the antenna, a bandpass filter, a low-noise amplifier, a down converter and an I-Q demodulator, in the reception chain, and an I-Q modulator, power amplifiers, bandpass filters and the antenna, in the transmission side. A diplexer separates transmission and reception paths. There are two D/A converters which generate the baseband analog signal using the samples at the output of the digital transmitter and two A/D converters which sample the I-Q analog signal that will be processed by the digital receiver.

We decided to implement two digital modems for experimental purposes. One is based on a single DSP chip and the other on a single ASIC (Application Specific Integrated Circuit). Both systems have the same functionality, but the programmable DSP allows to experiment with different algorithms.

The OBDH seen above controls the physical level of the communications and also implements upper level protocols for file transfers between the remote units and the Central Station.

In figure 8, we can see the modem block diagram. The modem is composed of a baseband modulation-demodulation part and some blocks which implement the channel coding functions of the modem. These blocks would be the scrambler-descrambler, the differential encoder-decoder and a convolutional encoder together with a Viterbi decoder.

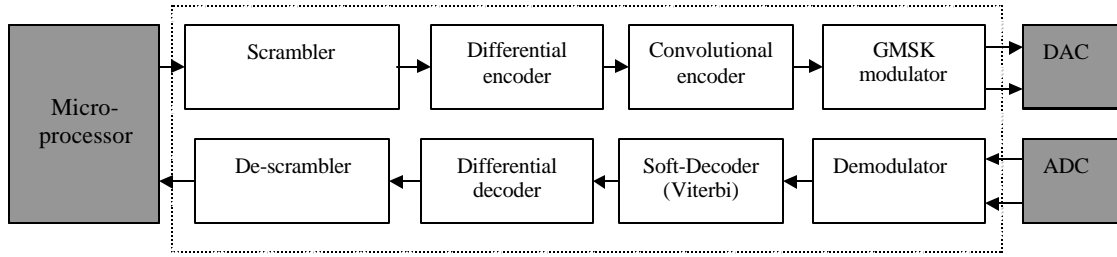


Figure 8. Modem block diagram

Modem Analysis

The modulation scheme used is a GMSK (Gaussian Minimum Shift Keying), as we have previously said. This modulation has good performance in satellite communications, allowing the use of high efficiency class C amplifiers (high power amplifiers, HPA).

CPM modulations not only provide constant envelope signals, but also continuous phase variations, which makes spectral sidelobes have less energy than those obtained in PSK schemes.

The CPM modulation is defined as:

$$x(t) = A \cdot \cos(\omega_0 t + \mathbf{j}(t) + \mathbf{q}) \quad (1)$$

where $A = \sqrt{2E/T}$ is the signal amplitude, ω_0 is the radian frequency of the carrier $\varphi(t)$ is the signal phase, which is a function of the time, and θ is a constant initial phase. The phase signal is:

$$\mathbf{j}(t) = \mathbf{ph} \sum_{k=-\infty}^n \mathbf{a}_k q(t - kT) \quad nT \leq t \leq (n+1)T \quad (2)$$

where $q(t)$ is the phase response and h is the modulation index, which gives the phase variations between two symbols. T is the symbol time, and α_k are the M-ary data symbols, which take values $\pm 1, \pm 3, \dots, \pm(M-1)$ (M is normally a power of 2). We have chosen GMSK modulation with parameter $h=1/2$, $M=2$ and $BT=0.3$.

We can implement this modulator in different ways, but the most general and straight forward way of implementing a robust CPM-transmitter is to use stored 'look-up tables'².

Figure 9 shows a general scheme of the receiver³. The channel bit rate is 24 Kbps, and the converters sampling rate is of 96 kHz, which makes 4 samples per symbol (bit). At the output of the filter, the samples are decimated to obtain 1 sample per bit. In addition, if we have introduced redundancy bits in the transmitter, we have to calculate their mean value, which corresponds to the individual repeated symbols. This is made at the output of the filter.

After the receiver filter, there is an AGC (*Automatic Gain Control*) to normalize the power of the signal used on carrier recovery loop.

Bit synchronization is carried out by interpolation techniques whose control is based on a zero crossing algorithm.

As was mentioned, the *carrier recovery* block must be able to track the high Doppler and its changes. Therefore, we must use two joined subsystems based on a second order loop with two detectors: the *Quadricecorrelator* allows synchronization when we have a high frequency error, and the *Rotational Phase Error Detector*, which follows fast frequency changes, based on previous decisions.

If we talk about the channel coding, we first have a *scrambler*, where we can find a classical self-synchronized scheme. The *differential encoder-decoder* tries to avoid phase ambiguities that could be present in carrier and bit synchronization.

The *convolutional encoder* used has as parameters (1, 2, 5), where $\frac{k}{n} = \frac{1}{2}$ is the code rate and $K=5$ is the 'constraint length', whose value was chosen as a trade-off between coding gain and computational complexity. We obtain with this encoder a coding gain of about 5 dB if we use a maximum likelihood receiver for the convolutional decoding. This kind of receiver can be implemented via the Viterbi algorithm with soft decoding.

All this channel coding is used to accommodate the signal to the channel features. As we have previously said, the modem bit rate is 24 Kbps with no coding, but this rate can be reduced to 12, 8, 4.8, 4 or 2.4 Kbps depending on the type of coding used.

Access techniques and frame and error control

Half-duplex communication has been used. Communication always takes place between the NANOSAT satellite and the earth stations. The satellite starts all dialogues with the earth terminals, so it must have information about the terminals which

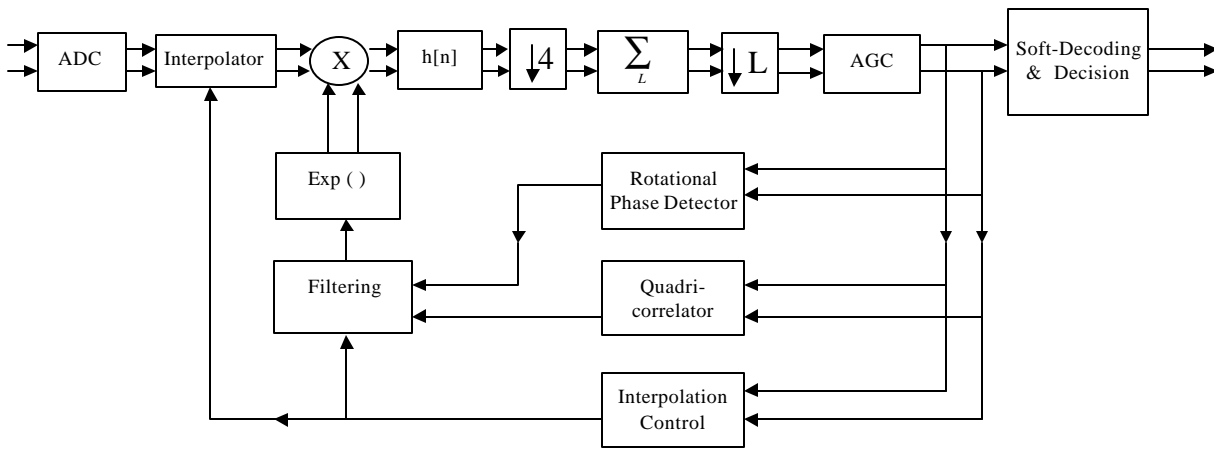


Figure 9. General receiver structure including carrier and bit synchronization

are visible at every time. This information is sent to the satellite by the Central Earth Station, where the satellite orbit is obtained periodically. Using this acknowledge and the coordinates of the fixed earth stations around the world, the Central Station calculates the intervals of time when each station is visible from the satellite, until the next time that this Central Station will be visible. The Central Station sends this information to the satellite.

All accesses are started with a periodic transmission of a specific signal by the satellite. After the transmission of this signal, the satellite establishes a number of access time slots, together with the stations that can send information in these slots.

Once the earth stations have received the initial signal, they send an access sequence with their address, the number of packets they want to send and additional information about the frequency error detected. Each access sequence must be transmitted in the slot assigned by the satellite. When NANOSAT has received this sequence, it will guarantee transmission and reception needs of the earth stations. Access sequence can also be used to obtain the relative position between the earth stations and NANOSAT satellite and improve time management and system capacity.

Earth stations can be classified according to two criteria: access velocity and access type. Then, there are fast and slow terminals if we look at the first criterion, or random or deterministic terminals for the second one. Mobile stations or first accesses of fixed earth stations use random accesses. These terminals send their access sequence by contention with a Slotted Aloha access type. In the case of a first access of a fixed earth station, its geographical coordinates are sent to the satellite. Then, the satellite will send to the Central Earth Station this information, to actualize its database of currently operative terminals. The position of deterministic earth stations

is known, and the satellite assigns one slot per known station, so that there is no collision between these stations.

There are four types of time slots, depending on the earth station. This type is based on the classification previously established. When the satellite has received the access sequence sent by the earth stations, it will transmit another sequence with the identified stations. Then, if a collision has taken place, all but one earth station involved in the collision must send its access sequence again. In this way, there is no need of specific procedures for detecting collisions in the satellite.

The information and signaling data is structured in packets. Each packet has an initial sequence for bit and carrier synchronization, which is called 'training sequence', a payload whose length depends on the type of packet, and a two bytes CRC field to allow error detection.

Antennas and RF subsystem

We have previously said that the attitude control of the satellite is based on the Earth magnetic field. As a result, the pointing direction of the satellite depends on its latitude. Therefore, NANOSAT antennas must be omnidirectional to cover the earth stations placed in all latitudes.

Due to the satellite dimensions, the omnidirectional pattern can be achieved at frequencies in the UHF or VHF bands with 4 inclined monopoles placed on the hexagonal facets. The final choice has been the UHF band because of the lower cost and size of the equipment in this band. Taking into account the set of frequencies allowed by the ITU (International Telecommunication Union), the chosen frequencies were 387.1 MHz for the downward link and 400 MHz for the upward link.

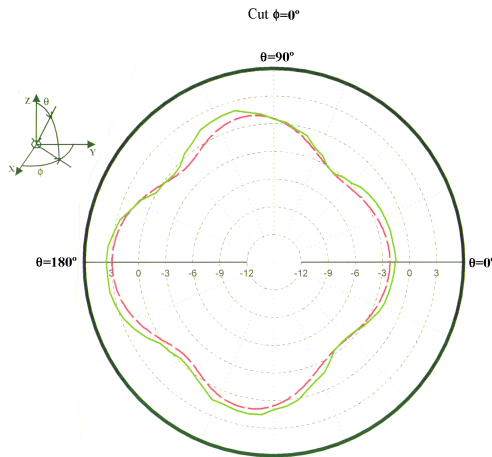


Figure 10. Radiation pattern (total power) of the NANOSAT antenna. Calculated (dotted-line) and measured (full-line)

In figure 10 we present the radiation pattern of the antenna (total power). It shows a gain of about 0 dBi with a ripple of ± 3 dB. The BFN (Beam Forming Network) feeds the monopoles with the same amplitude and phases of 0° , 90° , 180° and 270° to obtain RHCP (Right Hand Circular Polarization) around $\theta = 0^\circ$, LHCP (Left Hand Circular Polarization) around $\theta = 180^\circ$, and mainly linear polarization for intermediate directions.

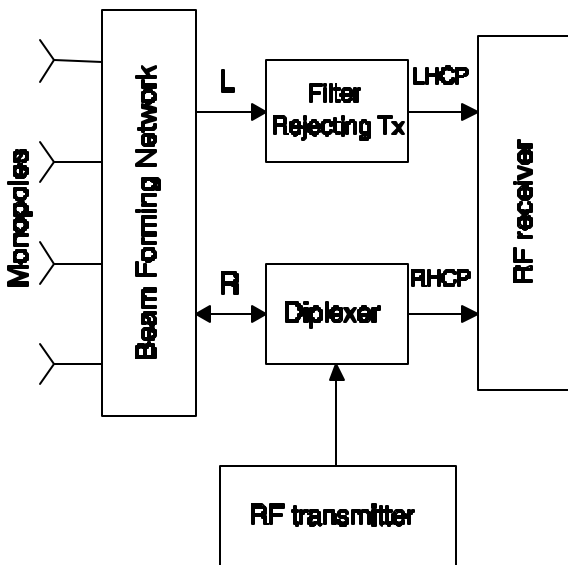


Figure 11. RF stage and antennas configuration

As it is shown in figure 11, two reception channels have been implemented in order to be able to receive any of those polarization, and a switch will select the channel in order to get a signal to noise ratio good enough for a correct reception. The receiver has, before the switch, a LNA (Low Noise Amplifier) in each channel, with a noise figure less than 1.2 dB. After down-conversion to the IF (70 MHz) and amplification, an I-Q demodulator supplies the I and

Q components of the signal to the modem. The decision of which channel must be selected in order to get a correct signal reception is taken by measuring the level of the in-quadrature (Q) signal and the noise at this point and by comparing its ratio to a reference level which will determine the switching moment.

On the transmitter side, the in-phase and in-quadrature components supplied by the modem are I-Q modulated with a quadrature modulator and up-converted directly into the final transmission frequency (387.1 MHz). The HPA is a MOS-FET amplifier which gives an output power of 5 Watts. This is enough power to allow communication with the earth stations for satellite elevations greater than 10° .

Power Supply Subsystem

We can begin our description of this subsystem with an estimation of the useful surface that faces the sun. Taking into account that the satellite will spin around its main inertial-momentum axis, the average surface orientated to the sun is 1386.3 cm^2 .

The solar cells we will use have a size of $20 \times 40 \text{ mm}^2$. With these cells, we obtain a maximum occupation factor of 54.1 %, or an effective surface of 750 cm^2 exposed to the sun. This is shown in figure 12.

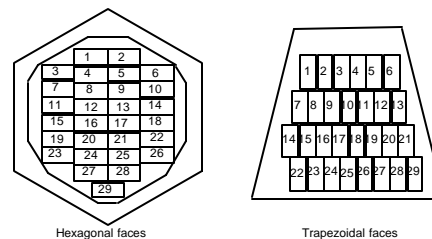


Figure 12. Solar cells distribution

All these cells generate an equivalent voltage of 23.9 V and a power supply of 17.0 W. These data have been calculated for an average operating temperature of 25° C . The energy generated and stored in the batteries must be enough to supply every subsystem inside the satellite, even when it is in an eclipse situation from the sun.

The chosen batteries are made of Ni-Cd and are qualified for operating in the space environment. Their capacity is 4.8 A-h @ 10° C . They must stand 16,500 charge-discharge cycles, which is a low earth orbit requirement. The batteries also have a depth of discharge (DOD) of 20 %. The batteries can be placed inside the satellite as two groups of eight or four groups of four batteries each. The operating temperature in space should be between 0 and $+5^\circ \text{ C}$,

whereas the storage temperature in Earth is between +6 and +3° C. Each of the 16 cells which compose the battery weighs 221 grams, and the dimensions are 80x67x54 mm.

There is a power saving mode when we do not have anything to transmit or receive. In those cases, we can switch off the communication subsystem (modem and radio frequency equipment).

The power supply subsystem has the ability to carry out telemetry functions and send control commands to respond to the previous measurements. The sampled signals are:

- Current through the battery: charge and discharge.
- Battery temperature.
- Bus voltage (battery).
- Relays status.
- Threshold voltage of the bus.

The control commands would be:

- Activate the drainage current in the cells.
- Activate-deactivate the power supply relays controlling the communication subsystem.
- Reset: switch off the ± 5 V and ± 12 V power supplies.
- Turn off the +12 V and +15 V power supplies.
- Switch on/off the experiments power supply.

Both the current and the temperature of the batteries are measured in two points and then averaged. We can classify the relays according to their functions in the power supply subsystem. Therefore, we have a start relay, which “switches on” the satellite when it is activated. We also have a power control relay to regulate the power flow to the experiments and radio frequency equipment.

Four fully qualified DC/DC converters from Interpoint have been used for power supplying the different subsystems. These converters give the voltages of +15, ± 12 , +5 and +8 Volts. The electrical noise generated by those converters is removed with two EMI (Electro Magnetic Interference) filters.

Experiments

Solar sensor

For the NANOSAT spacecraft, analog solar sensors (i.e. porous silicon (PS) based photodiodes) have been used with a twofold purpose: (a) to prove the feasibility in space environment of the implemented nanotechnology based on the elaboration of solar cells with a PS layer⁴, and (b) to provide spacecraft sun aspect angle determination for spin control.

The use of PS as an antireflection coating (ARC) together with its potential to texturize and passivate the silicon surface allows to simplify silicon solar cell processing schemes reducing three steps (texturization, passivation and ARC deposition) into one single step. For this purpose, PS based photodiodes ($5 \times 5 \text{ mm}^2$) were elaborated from p-type boron doped multicrystalline silicon wafers, with a resistivity of about $1 \Omega \cdot \text{cm}$. The n^+ emitter was formed by the thermal diffusion of phosphor. The PS layers were formed by chemically etching the emitter of the n^+/p junctions after deposition of the front and back contacts. An HF/ HNO_3 -based solution was employed at room temperature in the dark. The samples were rinsed in ethanol after the formation of the porous structure. This technique allows top contacts to be made directly onto the emitter, thus avoiding electrical conduction through PS which is a highly resistive material and shows poor electrical conductive properties.

The analog circuitry associated with each PS based solar cell is based on the use of an operational amplifier in order to get a voltage signal proportional to the short-circuit current of the device. All the electronic is mounted on one of the sides of a printed circuit board while the other side is used to place the PS based photodiode. This design allows a higher protection to the electronic components against the space environment, being the solar cell the only component directly exposed to the orbit radiation environment. For this reason, the PS based solar cells will be provided with a coverglass to reduce its degradation due to low energy proton particles.

Both the integrated circuit and the covered solar cell are encapsulated in a specially designed structure using aluminum black anodization and a specific baffling to provide a limited Field of View (FOV) for each solar detector.

Since the short circuit current and thus the output signal of each solar detector is proportional to the cosine angle of incidence of the solar radiation, the spacecraft spin axis determination is possible by using the output from three out of six PS based solar sensors positioned at different points on the spacecraft, and applying appropriate algorithms mainly based on the differential sun angle detector concept. This will allow to know the spacecraft nutation angle within 5° . Data acquisition for each solar detector will also be available to study the behavior of each device in a LEO space environment.

Laboratory tests have been performed under standard conditions of illumination (1 solar constant AM0) and temperature (25° C) in order to determine the electrical performance of the PS-based devices to be used as solar sensors for the NANOSAT mission. In particular, the electrical behavior of these devices

after long periods of atmospheric exposure as well as after extended photon irradiation (1 solar constant AM0, 25° C) has been found to be stable. The sinusoidal variation of the short circuit current of these devices with Sun angle from 0° C to 80° C was also confirmed. Furthermore changes of the solar sensor output with temperature within a range from 10° C to 80° C was determined. Both data are to be used in the algorithm implemented for spacecraft spin angle determination. It is foreseen to submit PS-based photodiodes to 1MeV electron irradiation at the three doses: (a) predicted dose for the envisaged application, (b) half that dose, and (c) twice that dose. An electrical characterization similar to that performed on non-irradiated solar sensor (i.e. beginning-of-life (BOL)) will complete all laboratory tests.

Finally, table I gives indication of the Qualification Test sequence. It must be pointed out that a special test bed will be designed for performance tests where the minimum configuration of three PS based solar sensors to determine the spacecraft spin angle is to be included.

Physical Measurements
Performance Tests
Vibration
Post-Vibration Performance Tests
Thermal Vacuum
Post-Thermal Vacuum Performance Tests
Thermal Cycling
Post-Thermal Cycling Performance Tests
EM Compatibility
Final Performance Tests
Final Inspection

Table 1. Qualification tests

The magnetometer

Another experiment related to nanotechnology is a magnetometer for the measurement of the satellite attitude. This will be done through the determination of the Earth's magnetic field. According to the mission specifications, it has a low mass (about 20 g for the sensor head and about 200 g for the control electronics) and low power consumption (less than 2 Watt).

The working principle of the magnetometer is the Faraday effect (rotation of the polarization plane of a light beam when passing through a medium influenced by an external magnetic field). The transducer material (Faraday rotator) for this sensor has been developed by us⁵ through a sol-gel method, resulting in a magnetic nano-composites of γ -Fe₂O₃/SiO₂. This material consists of isolated γ -Fe₂O₃ particles of nanometric size (average 20 nm) dispersed in a silica matrix. While bulk γ -Fe₂O₃ is a non-transparent ($\alpha \sim 10^4 \text{ cm}^{-1}$) ferromagnetic material

with no practical applications in the Faraday effect sensors, γ -Fe₂O₃ nanocomposites can present super-paramagnetic behaviors, large Faraday rotations (Verdet constant of about 4,000 rad/T.m) and moderate optical absorption ($\alpha \sim 70 \text{ cm}^{-1}$). Due to its large Faraday rotation we call to this material GFFR (Gamma Ferrite Faraday Rotator). Thanks to the former properties, we have successfully employed nano-composites of γ -Fe₂O₃/SiO₂ to measure magnetic fields of 1 mGauss in the range of ± 0.1 Gauss. The materials have been tailored for space applications and are under continuous development.

The structure of the sensor head (we call it Faraday modulus) is displayed in figure 13. A GFFR plate is stacked between a single polarizer and a set of four polarizers with their axis oriented at +45° and -45° with respect to the single one (polarimetric detection scheme). The light beam emitted by a LED is polarized and its plane rotates in the GFFR. This rotation is detected as an optical intensity change thanks to the stack formed by the four polarizers and the array of four detectors (quadrant photodiodes). The first prototype of Faraday Modulus looks like a button cell, with 20 mm of diameter and less than 5 mm of thickness. The Faraday Modulus contains several coils for the sensor self-calibration (in order to compensate the possible drifts of the Verdet constant due to the temperature and the wavelength).

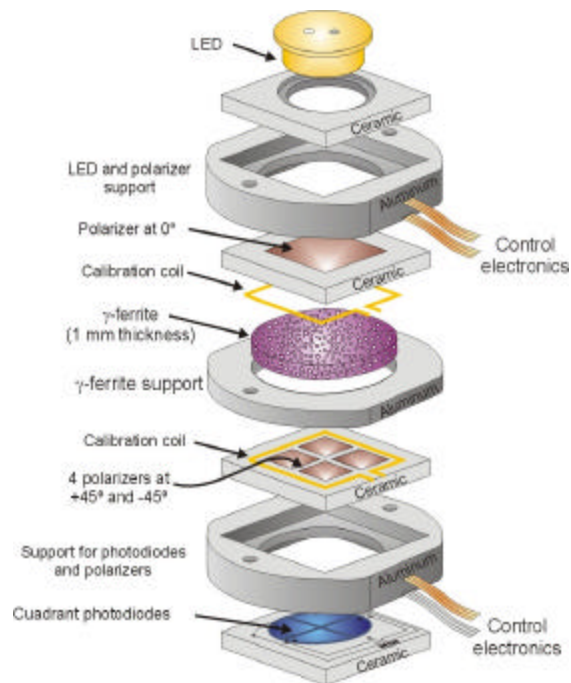


Figure 13. Sensor head structure

Control electronics contains a stabilized current source for the LED and a phase detection stage for the signal. As the NANOSAT has a certain spin, we will

use only two sensors for the determination of the magnetic field modulus and direction. The performance of this magnetometer is $6 \mu\text{V/nT}$.

Conclusions

We have presented in this paper the general design and development philosophy of a nanosatellite, called NANOSAT. It is not a question of size, mass or power consumption when we face to this kind of satellite. It is a different spacecraft philosophy.

We have described the OBDH, communication and power supply subsystems, as well as the experiments to carry out in this mission. These experiments will be based on nanotechnologies and will generate important data to be sent to the earth stations. A mailing service will be also implemented based on store-and-forward communications to allow messages transmission between the different earth stations.

NANOSAT is also intended to be used as a testbed for optical wireless links applied to intra-satellite communications⁶.

References

1. Laurent, P., "Exact and Approximate Construction of Digital Phase Modulations by Superposition of Amplitude Modulated Pulses (AMP)", IEEE Transactions on Communications, vol. COM-34, no. 2, February 1986.
2. Sundberg, C., "Continuous Phase Modulation", IEEE Communications Magazine, vol. 24, no. 4, April 1986.
3. Martínez, A., Rodríguez, S., Benavente, C., Muñoz-de-la-Torre, M.A., García, R., "Digital Implementacion of a Lineal Receiver for GMSK Modulation in a Communication Subsystem for a LEO Satellite", International Conference on Signal Processing Applications and Technology, DSP World and ICSPAT'99, Orlando, Florida, USA, November 1999.
4. Martín-Palma, R.J. et al., "Development and Characterization of Porous Silicon Based Photodiodes," Materials Science and Engineering: B, vol. 69-70, issue 0, 2000, pp. 87 – 91.
5. Guerrero, H., Rosa, G., Morales, M.P., del Monte, F., Moreno, E.M., Levy, D., Perez del Real, R., Belenguer, T., Serna, C.J., . Appl. Phys. Lett. 71 2698 (1997).
6. Guerrero, H., Arruego, I., Álvarez, M.T., Álvarez-Herrero, A., Levy, D., Torres, J., Santamaría A., López-Hernández, F.J., Hernanz, L.M.,

Barge, A., Huerta, R., Ferrer, C., "Optical Wireless Links for intra-Satellite Communications (OWLS)", 3rd Round Table on MNTs, ESTEC, ESA, Noordwijk, The Netherlands, May 2000.

Biographies

Mr. Ángel Martínez is a Telecommunication Engineer from the 'Universidad Politécnica de Madrid'(UPM), Madrid, Spain, since 1997. He is about to obtain a Ph. Degree on the same subject, specialized in Digital Signal Processing techniques applied to communications. He was given a grant for two years to work for the Universidad Politecnica de Madrid, where he took part in several projects related to the digital processing of voice signals and communications. He worked there for the European projects ISAEUS, to help deaf people to speak, the DIGISAT-S3M project, in cooperation with the company AMPER, and another communications project with the Spanish company SAINCO. He began to work at the UPM for the NANOSAT project, continuing his work since 1999 in the Space Science Division of the Spanish 'Instituto Nacional de Técnica Aeroespacial' (INTA) as hardware and software design engineer. He is in charge of the communication subsystem of the NANOSAT project.

Mr. Ignacio Arruego is a Telecommunication Engineer from the 'Universidad de Zaragoza', Zaragoza, Spain, since 1998. He worked for two years in BOSCH Y SIEMENS ESPAÑA (BYSE), between 1997 and 1999, as electronic hardware designer. Since september 1999 works at the Space Science Division of the Spanish 'Instituto Nacional de Técnica Aeroespacial' (INTA), where he is involved with the design of the RF subsystem for the NANOSAT program, and also works in a project for the European Space Agency (ESA) related to optical wireless links for intra-satellite communications. He collaborates with the "Agencia Nacional de Evaluación y Prospectiva" (ANEP), dependent of the Spanish Science and Technology Ministry, in elaborating an study about the optics research in Spain.

Mrs. Maria Teresa Álvarez has a M.S. degree (1989) in Electronic Physics from the 'Universidad de Santiago de Compostela', La Coruña, Spain. She worked for two years in digital electronics for INISEL and for three years as hardware designer in CRISA. She joined INTA in 1995 where she works in the Space Science Division involved with the NANOSAT project.

Dr. Jesús Barbero is a Telecommunication Engineer (Ph. Doctor) from the 'Universidad Politécnica de Madrid', Madrid, Spain (1968) and "Maître ès Sciences Aéronautiques" by ENSA (Paris 1969). He

joined the C.S.I.C. in Madrid in 1969. He has been involved in different projects, mainly with E.S.A. (European Space Agency) being in many cases the responsible of the electrical part of them. The subjects of those projects were Waveguide antennas (SAR, Windscatterometer,...), Printed antennas (SAR, Medium gain, Electronically Steerable...), and quasi-omnidirectional antennas for mobile communications. He joined INTA in 1996 being responsible of Antennas and RF subsystems of the NANOSAT project.

Dr. Héctor Guerrero has BSc. in Condensed Matter Physics (1988) and a PhD in Applied Optics (1992), both at Universidad Complutense of Madrid, Spain. He has been lecturing Physics and Optics at University for 10 years and last two has been at INTA. He is author of several papers, proceedings and reports in the field of optical fiber sensors, Faraday effect, plastic optical fibers, and Micro/Nano-Technologies for space applications.

Dr. David Levy graduated in Chemistry from The Hebrew University of Jerusalem (Israel), and started his work under the guidance of Prof. R. Reisfeld (M.Sc.) and Prof. D. Avnir (M.Sc. and Ph.D.), in 1982, 1984 and 1989, respectively, on the pioneering first application of the sol-gel process to the preparation of an organically doped silica gel-glass (1983). He was awarded the "*First Ulrich Prize*" for the most innovative work presented by a young scientist to the *VI International Workshop on Glasses and Ceramics From Gels* in 1991, and is author or co-author of over 70 papers and reviews in sol-gel doped photoactive/optical glasses and several application patents. His current research interest are optically active/photoactive organically-doped materials (bulk, thin-film and particles) and liquid crystal materials, by sol-gel processing and their applications. Also he is interested in space instrumentation and micro/nanotechnologies for space, focused on the specification, design, integration and qualification of a variety of optical instruments and materials, which are able to be implemented on the board of a satellite. He is currently associate research officer at the Instituto de Ciencia de Materiales de Madrid-ICMM, Consejo Superior de Investigaciones Científicas-CSIC, Madrid, and also is heading the Laboratorio de Instrumentación Espacial-LINES of the Area de Cargas Útiles e Instrumentación, División de Ciencias del Espacio of the Instituto Nacional de Tecnología Aeroespacial-I.N.T.A..

Mrs. Ana Gras has a M.S. (1981) degree in Astrophysics from Universidad Complutense in Madrid (Spain). After her graduation she obtained a fellowship from the Spanish Government to work at the Instituto de Energía Solar (IES) in Madrid. She has been involved in space solar cell testing since

1984 when she worked at the Solar Generators Section of the European Space Technology Centre (ESTEC) in the European Space Agency (ESA) for 18 months. She then joined the Spanish Space Agency INTA (Instituto Nacional de Técnica Aeroespacial) as technical responsible for setting-up SPASOLAB, ESA official laboratory for qualification and evaluation of solar cells for space applications to be operated by INTA. She has served at SPASOLAB as Test House Manager (THM) from March 1990 till September 1993 when she moved to USA and got a M.S. (1997) in applied physics from The John Hopkins University in Maryland (USA). She then returned to SPASOLAB at INTA. She is currently involved in SPASOLAB programs as terrestrial secondary calibration of solar cells and cascade solar cells testing. She also works in an experiment for the NANOSAT project to probe the feasibility of nanotechnologies in space environment implemented in a solar sensor.